Rheologica Acta Rheol. Acta 21, 464–469 (1982)

Elastic properties of polyethylene melts at high shear rates with respect to extrusion

H. M. Laun

Kunststofflaboratorium, BASF Aktiengesellschaft, Ludwigshafen/Rhein

Abstract: At high shear rates a steady state of shear flow with constant shear rate, constant shear stress, and constant recoverable shear strain is observed in the short-time sandwich rheometer after some few shear units already. The melt exhibits rather high elastic shear deformations and the recovery occurs at much higher speed than it is observed in the newtonian range. The ratio of first normal stress difference and twice the shear stress, being equal to the recoverable strain in the second-order fluid limit, significantly underestimates the true elastic shear strains at high shear rates. The observed shear rate dependence of shear stress and first normal stress difference as well as of the (constrained) elastic shear strain is correctly described on the basis of a discrete relaxation time spectrum. In simple shear a stick-slip transition at the metal walls is found. Necessary for the onset of slip is a critical value of shear stress and a certain amount of elastic shear deformation or orientation of the melt.

Key words: Polyethylene melt, recoverable shear strain, normal stress coefficient, extrudate swell, stick-slip transition

1. Experimental

A short-time sandwich rheometer (SSR) has been developed which makes it possible to measure time-dependent rheological properties like shear creep, stress relaxation, and elastic recovery in a homogeneous flow field up to high shear rates relevant to extrusion and injection moulding processes.

Two compression moulded sample films of equal thickness h = 0.2 to 2 mm are sheared in the gap between a central plate and a pneumatically driven cage (fig. 1). The whole sandwich is surrounded by a

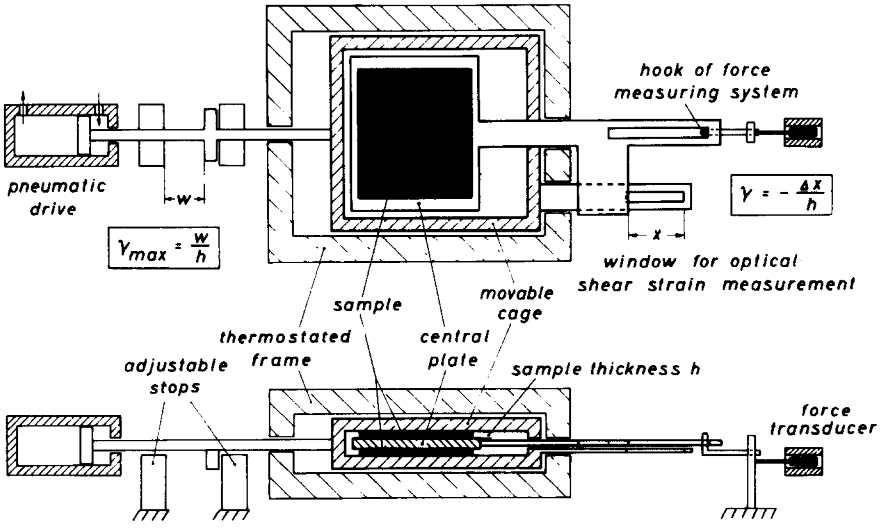

Fig. 1. Schematic drawing of the short time sandwich rheometer SSR

fix thermostated frame. In the shear creep test the cage is pulled to the left at constant force while the central plate is clicked into the hook of the force-measuring system. The shear strain γ is obtained from the relative displacement of central plate and cage. The force acting on the central plate gives the shear stress p_{21}. Evaluation of tests has been described in [1] for a low speed sandwich rheometer.

Parts of the central plate and of the cage are constructed such that they form a window which is illuminated from one side and the width x measured optically (Digital Dimension Meter 1000 C, Zimmer, Darmstadt). The time-dependent stress and strain are both recorded by a transient recorder of 0.1 ms resolution. Maximum force of the pneumatic is 500 N, maximum speed of the piston 1 m/s, maximum film area 0.02 m^2. The adjustable stop at the left makes it possible to suddenly stop deformation after a total strain $\gamma_{\max}$ to measure the relaxation of the shear stress. For recovery experiments, however, after a strain of $\gamma < \gamma_{\max}$ the cage is suddenly moved in reverse sense by the pneumatic till the right stop. Due to the slit in the central plate at the hook the central plate is released within much less than 10 ms. It can now move relative to the cage according to the elastic recoil of the sample. The optics measures the true strain independent of the position of the cage. A deformation of the sample during displacement of the whole sandwich due to inertia forces can be neglected.

The SSR enables high shear rate measurements of short duration. Hence, adiabatic heating can be shown to be less than 1 °C for the PE melts investigated here, even at the highest shear rates of 1000 s^{-1}.

Figure 2 shows a creep test followed by a recovery test. The short oscillation of p_{21} at the beginning of the test is caused by a short vibration of the whole

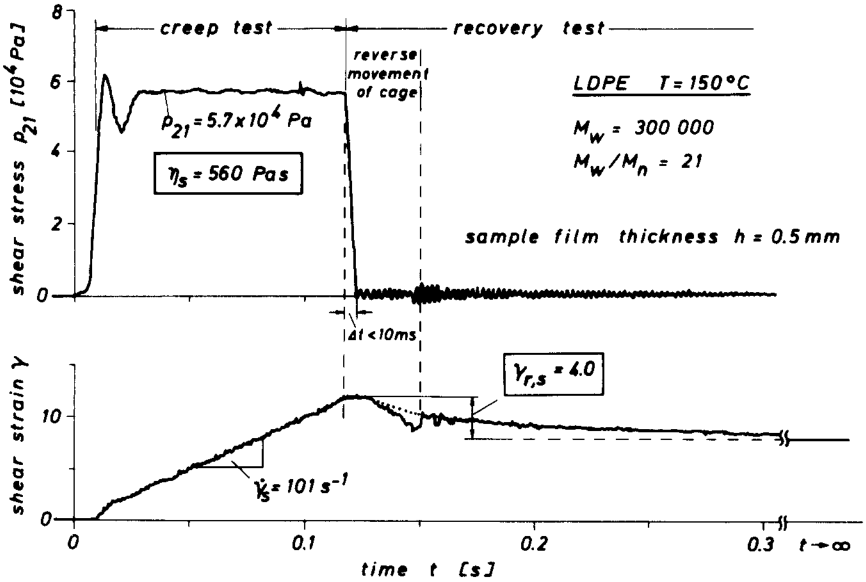

Fig. 2. Measurement of viscosity and elastic recovery

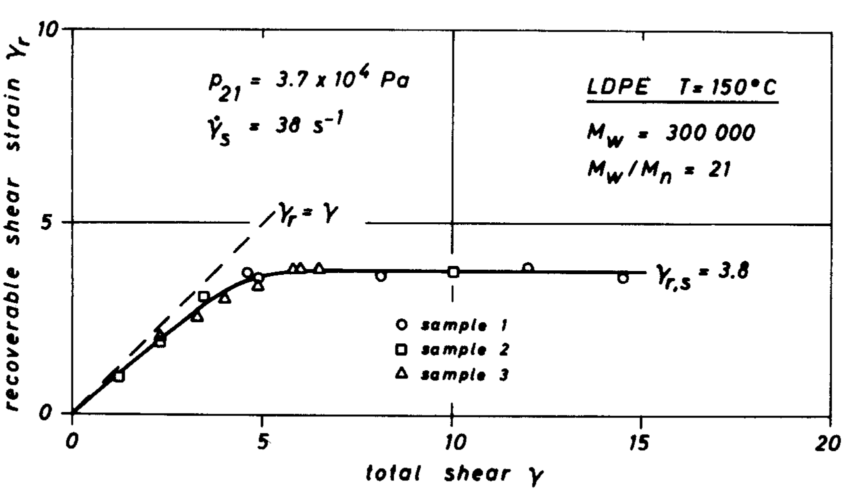

Fig. 3. Dependence of recoverable shear strain on total strain in a shear creep test

apparatus. After a small amount of shear the shear rate becomes constant and a steady shear flow is achieved. Having reached a total strain of about 12 the sample was unloaded by the reverse movement of the cage. The sample shows a rather fast elastic recovery. A recoverable strain of 4 is obtained within 1 s only, whereas in the newtonian range the total recovery would take several minutes!

During the fast reverse movement of the cage the optically measured strain is less than the true strain (dotted line) due to the time necessary for one scan over the window (1 ms). As the displacement of the cage is recorded, too, this effect can be corrected for.

During a creep test the recoverable strain increases with growing total strain in the first instance (fig. 3) and most of the strain is recoverable as indicated by the broken line of a completely elastic deformation. For a total strain bigger than five the recoverable strain becomes constant. This strain-independent value gives the steady-state recoverable strain $\gamma_{r,s}$. It should be noted that the total strain necessary to achieve a steady shear flow is strongly depending on the magnitude of $\gamma_{r,s}$.

2. Material functions in shear

In figures 4 and 5 experimental results obtained on two LDPE melts by three different apparatuses are compared. The material functions plotted versus shear rate are the steady-state values of viscosity, recoverable shear strain, and normal stress coefficient. Low shear rate viscosities were determined with a Weissenberg Rheogoniometer (WRG) modified by Meissner [2] (unfilled circles). In the high shear rate range a capillary viscometer was used (circles with tic). The viscosities obtained from the high speed sandwich SSR (full squares) are in very good agreement with the cone and plate and capillary data thus demonstrating the reliability of viscosity measurements with the SSR.

The second material function for which results from the SSR and the WRG can be compared is the steady-state recoverable shear strain. Recoverable strains at low shear rates can very accurately be measured by the servo-controlled WRG [2] (unfilled triangles). In the newtonian range $\gamma_{r,s}$ increases proportional to the shear rate [1, 3]. In the shear thinning range the increase becomes less pronounced. Unfortunately the speed of the servo-controlled WRG is not fast enough to give the true elastic strains after high shear rate tests which caused erroneous results earlier.

The recoverable strains from the SSR are represented by the full triangles. The WRG data agree with those in the overlapping range but only up to a shear rate of 0.1 s^{-1}. At still higher shear rates the WRG would give too small values. These results are not

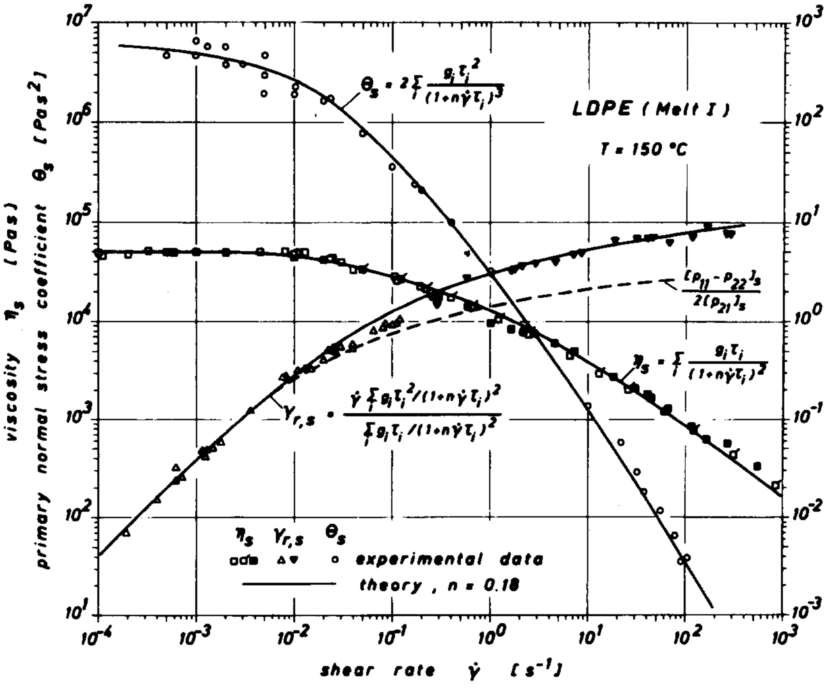

Fig. 4. Comparison of measured and predicted shear rate dependence of viscosity, normal stress coefficient, and recoverable strain is the steady state (LDPE melt, M_w = 300000, M_w/M_n = 21)

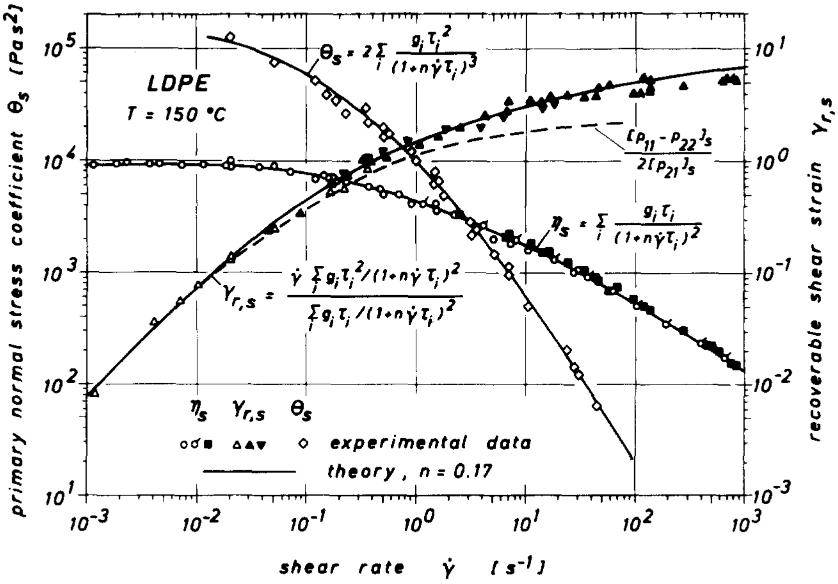

Fig. 5. Comparison of calculated and measured material functions is shear (LDPE Melt I)

contained in the figures for clarity. The recoverable shear strain measured on LDPE Melt I at 300 s^{-1} is 9. This magnitude is rather surprising.

The third material function, the normal stress coefficient, could be obtained from the WRG only (unfilled rhombs). Very often the ratio of first normal stress difference $[p_{11}-p_{22}]_s$ and twice the shear stress $[p_{21}]_s$ in the steady state is taken equal to the recoverable shear strain also in the non-newtonian range. The relation holds in the linear viscoelastic flow range of the melt [4]. From the measured normal stress coefficients and viscosities the stress ratio was computed. It is represented by the broken line. One can clearly see that the stress ratio significantly underestimates the true elastic strains up to more than a factor of two at high shear rates!

The full lines in figures 4 and 5 represent the theoretical predictions by means of a discrete relaxation time spectrum and an integral constitutive equation with strain-dependent and factorized memory function. The τ_i being the relaxation times and g_i the corresponding relaxation strengths. The nonlinearity of the flow behaviour is introduced by the so called damping constant n following Wagner [5]. Whereas the analytical expressions for the viscosity and the normal stress coefficient have been published earlier [6], the theory for the recoverable shear strain was recently worked out in collaboration with Fischer [7]. The agreement between experiment and theory over more than 6 decades of shear rate (Melt I) is very encouraging.

3. Stick-slip transition of HDPE

Linear polyethylene melts of high molecular weight exhibit a drastic increase of flow rate if the extrusion pressure reaches a critical value. It is assumed that this spurt effect is caused by a stick-slip transition at the die wall [8]. The low molecular weight PE in figure 6 does not show a flow instability up to 1000 s^{-1}. Compared with the long chain branched polyethylenes of similar viscosity (fig. 5) the linear melt shows significantly smaller recoverable strains. Contrary to the low viscosity HDPE the high molecular weight HDPE exhibits a pronounced flow instability for wall shear rates $\dot\gamma \gtrsim 250$ s^{-1}. Up to that shear rate agreeing results from the cone and plate, capillary, and sandwich rheometers are obtained.

The recoverable shear strain of the high molecular weight HDPE remains nearly constant over the shear rate range investigated, the highest recoverable strains being about 3. The data points in the vicinity of the instability region are represented by stars as in fact they are no true steady-state values.

Figure 7 shows the shear stress and the apparent shear strain – as calculated from the relative displacement of cage and central plate – versus time. This quantity only gives the true shear strain as long as the melt sticks at the wall. A black coloured mark in the sample films was used to make the true shear deformation visible. The sample was sheared up to different amounts and then was cooled down under shape constrain in order to take photographs of the flow profiles. The arrows indicate the corresponding parts of the test where the sample was frozen in.

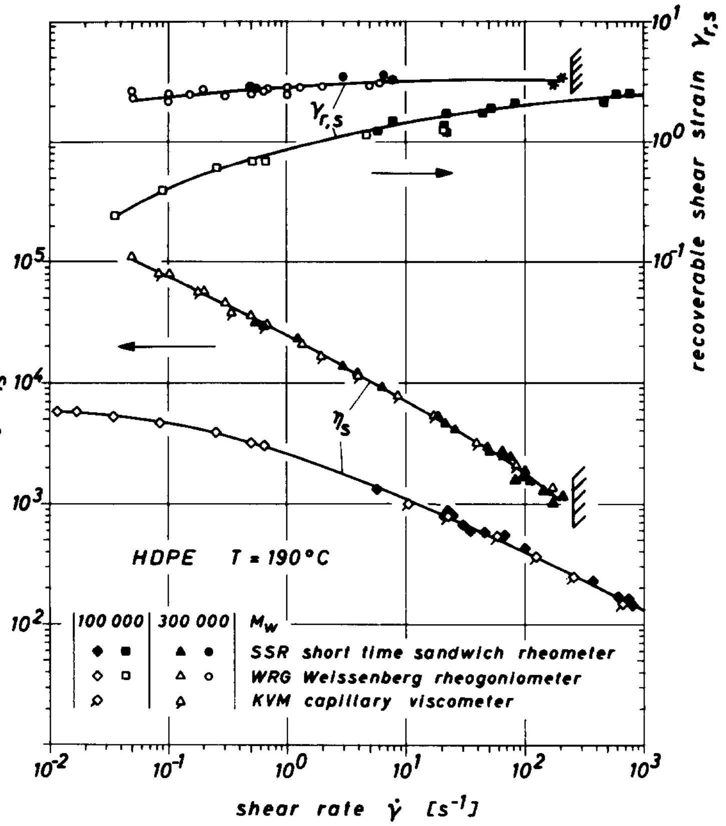

Fig. 6. Viscosity and recoverable shear strain of HDPE melts

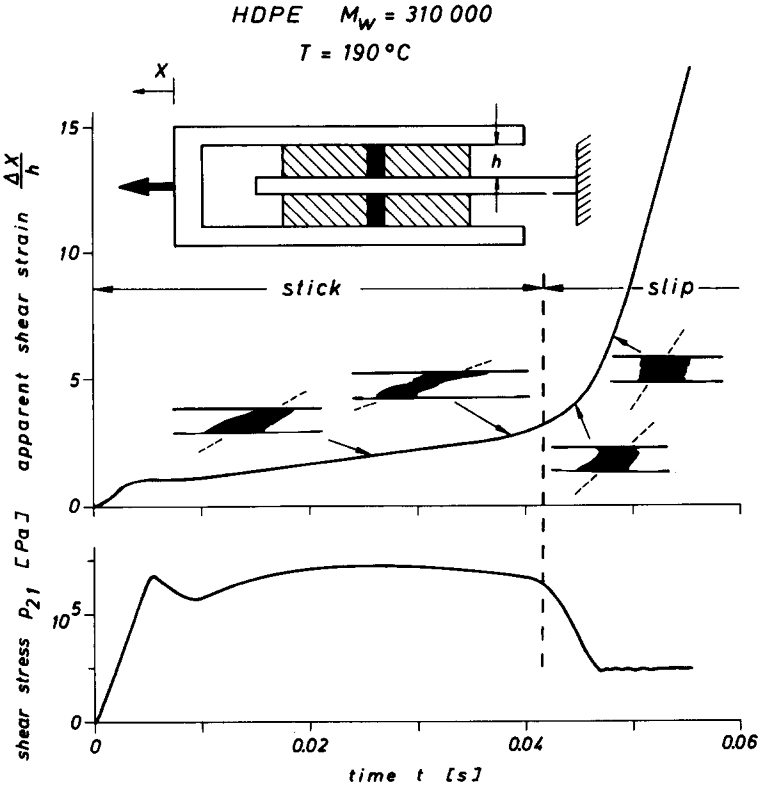

Fig. 7. Stick-slip transition of a HDPE melt in the sandwich rheometer

After approximately 10 ms a nearly constant shear stress acting at the melt and a nearly constant apparent shear rate is observed. The sample sticks at the metal plates and is deformed as expected. This is evident from the inclination of the flow profiles.

After a certain shear deformation, however, the stress transmitted to the central plate decreases suddenly and the apparent shear rate increases very rapidly. The flow profiles show that now slip occurs at the metal plates. During this period the shear deformation imposed in the stick phase recovers nearly totally such that the sample finally appears nearly undeformed! That means that the preceding shear deformation has been essentially elastic. It can be concluded that for the stick-slip transition not only a critical shear stress but also a certain amount of (elastic) shear deformation or orientation of the melt must be achieved.

4. Extrudate swell and elastic shear strain

Extrudate swell of a long die is unquestionably attributed to the elastic shear strains built up within the die [4]. We can measure extrudate swell B of long dies, calculate the corresponding true wall shear rate $\dot{\gamma}_w$ and compare extrudate swell with the recoverable shear strains measured in the sandwich at the same shear rate. This is a recommendable procedure to examine expressions interrelating extrudate swell and recoverable shear strain. The table gives a compilation of data obtained on Melt I at 150 °C.

Extrudate swell for dies with a length over radius ratio of $L/R = 60$ was measured on annealed samples. The influence of interfacial tension has been corrected for [9]. The values are only slightly higher than those of a die of $L/R = \infty$. At a wall shear rate of 144 s^{-1} where the measured recoverable strain was 8.1 the stress ratio only had a value of 2.7. Therefore, if the elastic strain is replaced by the stress ratio the magnitude of predicted extrudate swell would be significantly smaller.

Table

$\dot{\gamma}_w$ [s^{-1}]	B ($L/R = 60$)	$\gamma_{r,s}$	$\frac{[p_{11} - p_{22}]_s}{2[p_{21}]_s}$
0.107	1.28	1.3	0.76
1.19	1.50	3.2	1.5
13.0	1.67	5.5	2.2
144	1.73	8.1	2.7

References

1. Laun, H. M., J. Meißner, Rheol. Acta **20**, 211 (1981).
2. Meißner, J., Rheol. Acta **14**, 201 (1975).
3. Laun, H. M., Colloid & Polymer Sci. **259**, 97 (1981).
4. Lodge, A. S., Elastic Liquids (London-New York 1964).
5. Wagner, M. H., Rheol. Acta **15**, 136 (1976).
6. Laun, H. M., Rheol. Acta **17**, 1 (1978).
7. Laun, H. M., E. Fischer, to be published elsewere.
8. Uhland, E., Rheol. Acta **18**, 1 (1979).
9. Laun, H. M., H. Münstedt, Rheol. Acta **17**, 415 (1978).

(Received April 28, 1982)

Author's address:

Dr. H. M. Laun
Polymerphysik, Festkörperphysik – G 201
Kunststofflaboratorium
BASF Aktiengesellschaft
D-6700 Ludwigshafen/Rhein